Geophysically-derived temperature and crystal fabric constrain past and present ice-sheet dynamics

Overview. The greatest uncertainty for projections of future sea level rise is ice-sheet dynamics and the potential realization of theorized instabilities (Fox-Kemper et al., 2021). While knowledge on the precise fate of Earth's ice sheets is still out of reach, looking to past states could provide insight on their potential evolution. Past ice-sheet states and particularly their dynamics are preserved in present-day ice-temperature deviations (Robin, 1955) and preferred crystal orientation fabric (COF) (Alley, 1988); moreover, the future ice dynamics are governed by those same properties through the ice viscosity (Azuma, 1994; Glen, 1955) and ice sliding over a temperate bed (Lliboutry, 1968; Weertman, 1957). Theoretically, ice temperature and COF can both be measured using the amplitude and phase information from a reflected radar wave (Fujita et al., 2006; MacGregor et al., 2007), but prior work shows that it is notoriously difficult to disentangle these intrinsic properties of the ice column from each other or even from interface properties such as reflectivity between layers and at the ice-sheet bed (e.g. Holschuh et al., 2016). Here, I outline my proposal to contribute incremental development of the methods for radar power/phase interpretation and to use them alongside process-scale models to infer both present-day and paleo ice-sheet dynamics. I focus on three regions of the Antarctic Ice Sheet: The Siple Coast, South Pole Lake, and Hercules Dome, with the specific scientific problem being different for each.

1. Background

Ice-sheet history is commonly inferred using numerical models (DeConto and Pollard, 2016), using proxies from the underlying geology (Brook et al., 1996) and sediment (Venturelli et al., 2020), and using ice stratigraphy as surveyed with geophysical tools (MacGregor et al., 2015a). Direct measurements of physical properties from ice cores, as opposed to proxy records, have also been used to infer ice-sheet history including borehole thermometry (Dahl-Jensen et al., 1998) and thin sections of the COF (Alley, 1988). Here, I focus on how those physical properties can be inferred remotely with ice-penetrating radar and what we can learn about ice-sheet history without direct sampling or in-situ instrumentation. In this section, I overview the current glaciological theory for both ice temperature and COF. Then, I discuss the influence each has on the electrical properties of ice and how they can be measured remotely using ice-penetrating radar.

1.1 Ice Temperature

Temperatures of glacier ice range from temperate to ~-60°C, which corresponds to a viscosity range over three orders of magnitude (Glen, 1955). Ice is generally warmest at the glacier bed, being heated from below by the geothermal flux, and coldest near the surface where ice is in equilibrium with the mean air temperature. Heat transfer between those two boundaries is modeled as an advection-diffusion problem with heat generation by strain (Clarke et al., 1977) and in some cases liquid water infiltration (Phillips et al., 2010). Because the length scale for thermal diffusion in ice is long, deviations in ice temperature can be preserved for thousands of years (Figure 1A).

Near an ice divide, heat sources are weak and advection is predominantly vertical with a velocity profile that is relatively well understood (Lliboutry, 1979). Therefore, strong inferences can be made for the unknown parameters at the boundaries. For instance, climate history is inferred using borehole thermometry (Dahl-Jensen et al., 1998), and geothermal flux is constrained at locations where the thermal state of the bed is known to be either frozen or thawed (Fudge et al., 2019).

Away from the ice divides, flow speeds generally increase meaning that the strain heat source is stronger, and that longitudinal/lateral advection more heavily influence temperature. Longitudinal advection is generally under-appreciated in simple temperature models (c.f. Dahl-Jensen, 1998; Weertman, 1968) but has been observed in locations with fast flow and a strong surface temperature gradient (e.g. Harrington et al., 2015; Iken et al., 1993). Lateral advection is important along ice-stream shear margins where a strong lateral temperature gradient forms. Theory on shear-margin temperature comes from a few isolated measurements in the Siple Coast Ice Streams (Engelhardt, 2004) as well as thermodynamic models of varying complexity (Jacobson and Raymond, 1998; Meyer and Minchew, 2018; Perol and Rice, 2015; Suckale et al., 2014). Despite the efforts to build a theoretical understanding, these models are likely still underestimating the importance of both vertical (Holschuh et al., 2019) and longitudinal advection.

1.2 Crystal Orientation Fabric

Snow crystals are deposited at random orientation on the glacier surface, meaning the COF is initially isotropic. As ice flows, crystal c-axes rotate away from the primary extensional axis and toward compression (Figure 1B) (Alley, 1992). Single-pole fabrics with upward-pointing c-axes develop at an ice dome where flow is by uniform vertical compression and outward extension in all directions from the dome. In this case, the ice hardens in the vertical and preserves old ice near the bed (Raymond, 1983). Girdle fabrics develop in various ice-sheet settings, with the precise orientation and quality differing for each. Along an ice divide, where there is one prominent extensional direction, a vertical girdle develops perpendicular to the axis of extension (Young et al., 2021). The center of an ice-stream is similar, with extension in the direction of ice flow (Smith et al., 2017). A partial horizontal girdle develops in an ice-stream shear margin where transverse shear dominates.

The COF strength depends on the total strain accumulated over time, $\epsilon = \dot{\epsilon}t$. Laboratory studies show that cumulative crystal reorientation is sufficient to effect subsequent deformation by cumulative strain ~0.1-0.15 (Budd and Jacka, 1989). Therefore, vertical strain rates at an ice dome or ice divide, ~10^{-5}-10^{-4} yr^{-1}, would develop a recognizable COF on the order of thousands to tens of thousands of years. In areas with much higher strain rates such as an ice-stream shear margin, ~10^{-2}-10^{-1} yr^{-1}, the COF develops much faster, even on the order of years. An established COF in a shear margin can further soften the ice and promote faster flow (Jackson and Kamb, 1997). Laboratory studies show that ice is at least two orders of magnitude stiffer along the crystal c-axis (Shoji and Langway, 1988).

1.3 Radar Power and Phase Interpretation

Theoretically, ice temperature and COF can both be measured without drilling into the ice by interpreting their effect on the measured power (attenuation) and phase (birefringence) from ice-penetrating radar. Radio waves are attenuated in ice primarily by electrical conduction. Protons are the charge carrier, so conduction is facilitated by the movement of protonic defects in an imposed electric field (Figure 2A). As a radar wave propagates through the crystal, its power is attenuated more if proton conduction is more efficient; that is, if there are more free charge carriers (more ions), adequate lattice positions to accommodate charge conduction (more defects), or more energy available for molecular rotations (higher temperatures). Over small areas (10s to 100s km^2), any measurable change in radar attenuation is most likely associated with contrasts in ice temperature (e.g. MacGregor et al., 2015b; Schroeder et al., 2016).

Ice permittivity is anisotropic (Fujita et al., 2000), so radio waves propagate fastest when their polarization aligns with the crystal c-axis (Figure 2B). Bulk permittivity is then dependent on the aggregate orientation of ice crystals (the COF) and the wave polarization relative to that COF. For instance, a girdle fabric induces a measurable phase delay between radar acquisitions polarized parallel vs. perpendicular to the girdle, with the magnitude of the phase gradient correlating to the strength of the girdle (Jordan et al., 2020). When polarized oblique to the girdle, the wave 'turns' as it propagates through the ice. That is, an initially linearly polarized wave transitions to circular (or elliptic) polarization. The instrument orientation at which no 'turn' is observed (cross-polarized extinction) is then aligned with the girdle orientation (Ershadi et al., 2021). In theory, wave reflection properties (scattering) can also be anisotropic (Drews et al., 2012), possibly causing an abrupt phase transition in the received waveform. Below, I focus on steady phase gradients which should be minimally affected by anisotropic scatterers.

2. Proposed Projects

In what follows, I describe the work that I have done up to now on methods development as well as three proposed investigations which apply those methods. Each of the proposed projects has at least some preliminary results, with the first two being significantly more developed than the third.

2.1 Methods Development

Deliverables: *One lead-author (Hills et al., 2020) and one coauthor manuscript (Lilien et al., 2020)*

Within the glaciology community, radar processing flow is generally inconsistent between and even within groups. It is often difficult to decipher how one dataset was processed compared to another. In an effort to standardize processing, we created ImpDAR (Lilien et al., 2020), a free, open-source, and pip-installable Python library. ImpDAR is compatible with many of the commonly-used radar systems including PulseEKKO, GSSI, etc., as well as some custom data formats such as the Gecko software used for high-frequency systems (e.g. Welch and Jacobel, 2005, 2003). Within ImpDAR, we are building the tools for power and phase interpretation mentioned above. A framework for empirical attenuation measurements was designed by Hills et al. (2020) and all methods are included in ImpDAR. Processing flows for Autonomous phase-sensitive Radio Echo Sounding (ApRES) measurements (Nicholls et al., 2015) of both vertical motion (Brennan et al., 2014) and polarimetry (Jordan et al., 2019) are being added to ImpDAR as well.

2.2. Study 1 – Siple Coast Ice Streams

Deliverables: *One lead-author manuscript (Hills et al., in review)*

Recent studies suggest that plane-shear strain in ice-stream shear margins warms ice to its melting temperature through as much as half of the ice column (Meyer and Minchew, 2018; Perol and Rice, 2015), this excessively warm ice being necessary to match the high strain rates measured in surface velocities (Suckale et al., 2014). However, in-situ measurements of ice temperature from hot-water boreholes (Engelhardt, 2004) and radar attenuation (Figure 3) (Christianson et al., 2016, 2012; Jacobel et al., 2009) each suggest independently that temperature in the Siple Coast Ice Streams is in fact *colder* than the surrounding slow-flowing ridges. Even measurements directly from the Dragon Shear Margin of Whillans Ice Stream (Harrison et al., 1998) are ~10°C colder than suggested by the analytical solution for shear margin temperature (Meyer and Minchew, 2018).

Hypothesis: *Longitudinal temperature gradients in the Siple Coast ice streams are a sufficiently strong advective heat sink as to compete with heat production in the shear margins, requiring an alternative weakening mechanism to match the measured strain rates.*

I propose a two-fold approach to address ice-stream and shear-margin temperatures throughout the Siple Coast Ice Streams. First, I summarize the attenuation calculations from prior ground-based radar surveys (e.g. Christianson et al., 2016; Jacobel et al., 2009), applying various methods from the framework we developed for empirical attenuation (Hills et al., 2020). While these attenuation results have been presented past studies, they have been in the context of a local interpretation or as a correction to bed-reflectivity analysis. Second, I add a longitudinal advection parameterization to the standard advection-diffusion thermal model to directly compare how this advective heat sink competes with in-situ heat generation from vertical shear near the ice-bed interface and plane shear in the lateral shear margins. I use standard data products to calculate longitudinal advection for three ice-stream catchments (Figure 3) and compare the model result to borehole temperature measurements (Engelhardt, 2004; Harrison et al., 1998).

2.3. Study 2 – South Pole Lake

Deliverables: *One lead-author manuscript (Hills et al., 2022)*

The history of ice-sheet dynamics in the South Pole sector through the glacial transition are actively debated. An initial theory was based on temperature measurements from the AMANDA and IceCube projects (Price et al., 2002), stating that the deep ice is too cold for a thawed bed despite prior airborne radar observations of the nearby South Pole Lake (SPL) (Carter et al., 2007). Price et al. (2002) suggested that the lake had completely frozen and that the observations were a 'fossil' of the prior ice sheet. While active-source seismics have since confirmed that the lake persists today (Peters et al., 2008), Beem et al. (2017) argued that the presence of liquid water is not incompatible with the cold temperature measurements. They insist that the lake was created during the last glacial period (~14 thousand years ago) when the Support Force Ice Stream extended into this region and increased heat production to melt the lake. Their interpretation of a paleo ice stream is in line with prior radar surveys collected in this area based on both submergence rates (Beem et al., 2017) and internal layer disruptions (Bingham et al., 2007). A secondary theory for South Pole dynamics contradicts the first. Lilien et al. (2018) compared historical accumulation rates collected from the South Pole Ice Core to accumulation rates from an upstream radar survey, finding that this ice has actually been thickening and speeding up through the Holocene.

Hypothesis: *The South Pole region of interior East Antarctica is thermodynamically stable in the present-day ice dynamic regime and has been through at least the last interglacial. South Pole Lake is therefore a viable target for subglacial sediment sampling.*

I propose an integrated approach where the historical thermodynamics and the present-day ice dynamics are tied together into a single interpretation. None of the prior studies used historical data to constrain their temperature modeling, but newly available data from the South Pole Ice Core make this possible. I use accumulation and temperature proxy data from the ice core (Kahle et al., 2021) as boundary conditions for a 1.5-dimensional model of ice temperature through time (*model from Study 1*). I optimize the modeled geothermal flux so that the output most closely matches present-day ice temperature measurements from IceCube (Price et al., 2002) and a temperate bed for the measured ice thickness, assuming regional melting.

In addition to the temperature modeling, we have conducted the most comprehensive geophysical survey to date of SPL (Figure 4) to understand its present-day dynamic setting which also provides a constraint on the thermodynamic history. We mapped the surface elevation using kinematic GPS, mapped the ice stratigraphy and ice thickness using deep-sounding radar, measured vertical ice motion at 10 locations on and off the lake using ApRES, and measured horizontal ice motion at 50 locations on and off the lake using precision GPS. We find that the lake is currently full to its capacity, implying that significant basal freeze-on through the Holocene is unlikely. Our horizontal and vertical strain measurements also indicate that basal sliding is likely occurring today, consistent with a regionally thawed bed.

2.4. Study 3 – Hercules Dome

Deliverables: *One lead-author manuscript (targeting TC or JGR) and various coauthors*

Hercules Dome (HD) lies in the bottleneck between the East and West Antarctic Ice Sheet (WAIS). It is sufficiently proximal to the WAIS that an isotopic record of hypothetical WAIS collapse during the last interglacial period (~120 ka) could be preserved in the deepest ice (Steig et al., 2015). In a recent study, we demonstrated high likelihood that ice from the last interglacial period is preserved at the grid-westernmost extent of HD with signs of a frozen bed and stable divide flow through measurements of a Raymond effect (Fudge et al., in prep). However, it is not clear how past transitions in ice flow and divide migration may affect ice-core interpretation. This is made especially clear by evidence of past streaming flow preserved in bedrock troughs beneath the grid-eastern portions of HD (Hoffman et al., in prep).

Hypothesis: *The present-day surface geometry of Hercules Dome, a triple divide, is consistent with historical ice dynamics since the last interglacial, and cumulative strain during those ~120 ka is preserved in the present-day COF.*

I propose a survey of quad-polarized (quad-pol) ApRES acquisitions at HD with the intent to survey the dome's COF for past and present flow patterns. Unlike multi-polarization methods (e.g. Jordan et al., 2020) which use a series of co-polarized acquisitions at varying azimuth, quad-pol acquisitions use the cross-polarized terms in a rotational transform (Young et al., 2021). Therefore, the orientation and magnitude of a girdle fabric can be isolated by cross-polarized extinction and co-polarized phase delay, respectively.

During the 18-19, 19-20, and 21-22 HD seasons, we conducted quad-pol acquisitions at a total of ten sites which form an 80-kilometer transect along the predominant E-W divide, a 10-kilometer transect which crosses the divide, and two acquisitions on the South Ridge extension (Figure 5). At each acquisition location, the quad-pol data will be translated to depth profiles of x-y COF orientation and strength by optimizing to a layered effective-medium model (Ershadi et al., 2021). The resulting COF orientation and strength profiles across the dome will be interpreted in the context of the present-day surface strain rates measured with repeat GNSS acquisitions and vertical strain rates measured with repeat

ApRES acquisitions. The consistency, or lack thereof, between COF results and present-day ice dynamics will be used to investigate the likelihood of divide migration through time.

3. Summary and Outlook

Through the first half of my PhD, I built knowledge on glacier thermodynamics, ice physics, and radar theory. Much of my research has been dedicated toward developing tools for radar processing. Into the remainder of my PhD, I will apply those tools to the three scientific problems laid out above. For *Study 1 – Siple Coast,* no new data are needed, the analysis is finished, and the manuscript has been submitted for review. For *Study 2 – SPL,* all of the data have already been collected and archived, and the manuscript has already been accepted for publication. For *Study 3 – HD,* the necessary data have been collected and initial analysis has been done. Near-term objectives are to develop the effective medium model and constrain depth profiles of COF orientation and strength at each quad-pol location. The finishing work on this project will be completed after the next field season ('22-'23) when the repeat acquisitions can be made at all locations.

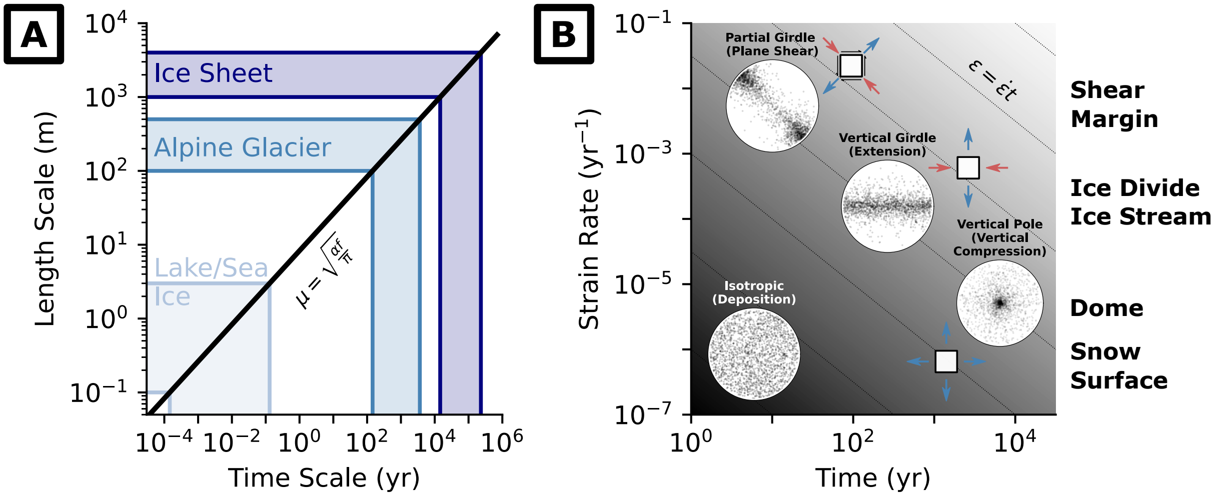

Figure 1. *Relevant process timescales in ice. A) The characteristic length scale for thermal diffusion, μ, is dependent on the temporal frequency of the temperature change, f, and the thermal diffusivity of ice, α. B) Crystal reorientation is a result of cumulative strain, $\epsilon = \dot{\epsilon}t$, so the quality and strength of a crystal fabric depend on the spatial pattern of local strain rates and the total time over which those have been stable.*

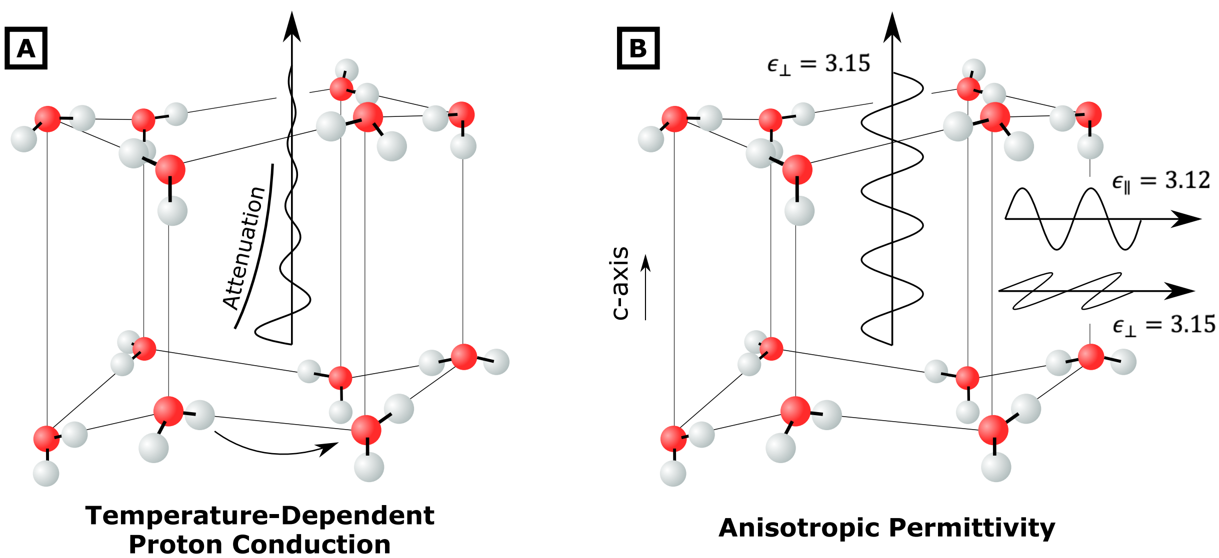

Figure 2. *An illustration of radar attenuation (A) and birefringence (B) at the molecular scale. Protons (white spheres) move between molecules in an imposed electric field. Electromagnetic wave speeds $\left(\frac{1}{\sqrt{\epsilon}}\right)$ are slightly faster when polarized parallel ($\epsilon_{\parallel}$) to the c-axis than perpendicular ($\epsilon_{\perp}$).*

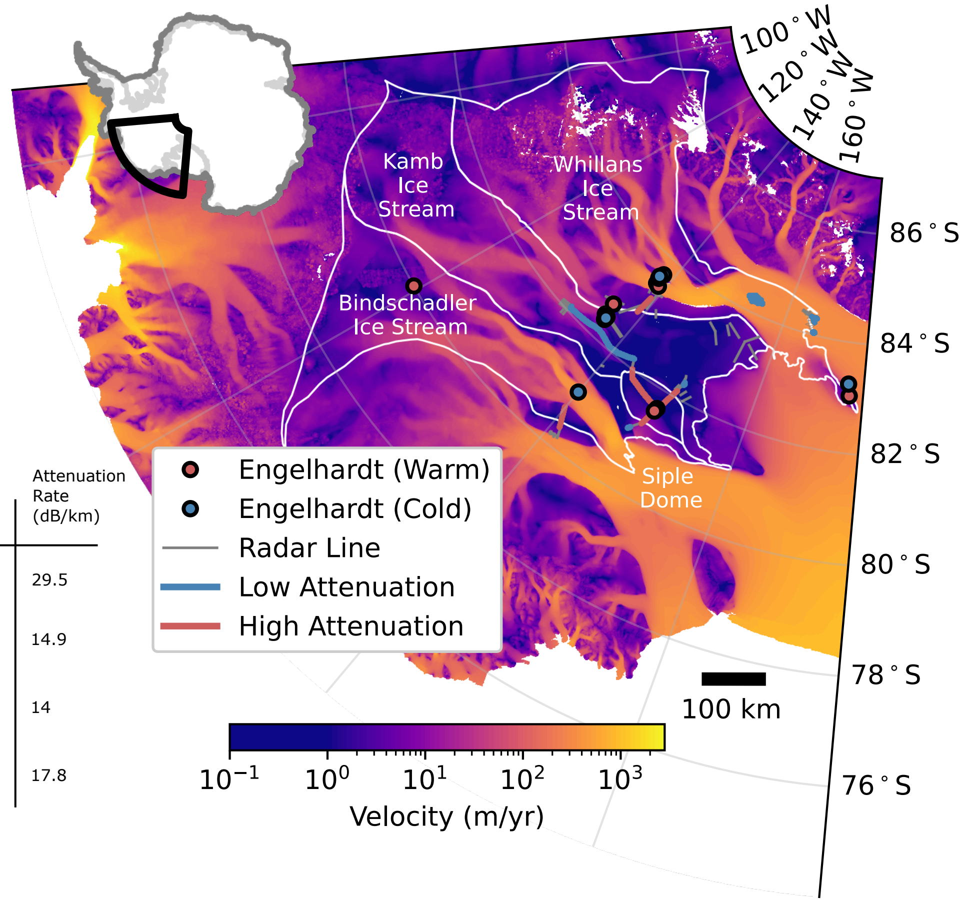

Location	Attenuation Rate (dB/km)
Siple Dome	29.5
Kamb Ice Stream	14.9
Whillans Grounding Zone	14
Subglacial Lake Whillans	17.8

Figure 3. *Data and radar analysis summary of Study 1 – Siple Coast Ice Streams. The colormap shows Ice surface velocity at the (Mouginot et al., 2019). Dots mark borehole drilling locations colored to indicate whether the measured temperature profile is relatively cold (blue) or warm (red) based on the original distinction (Engelhardt, 2004). Lines correspond to the radar profiles collected in previous studies. Drainage areas of the Bindschadler, Kamb, and Whillans ice streams (Rignot et al., 2013) are outlined in white, as is Siple Dome. Table) Attenuation rates from ground-based radar studies in this region.*

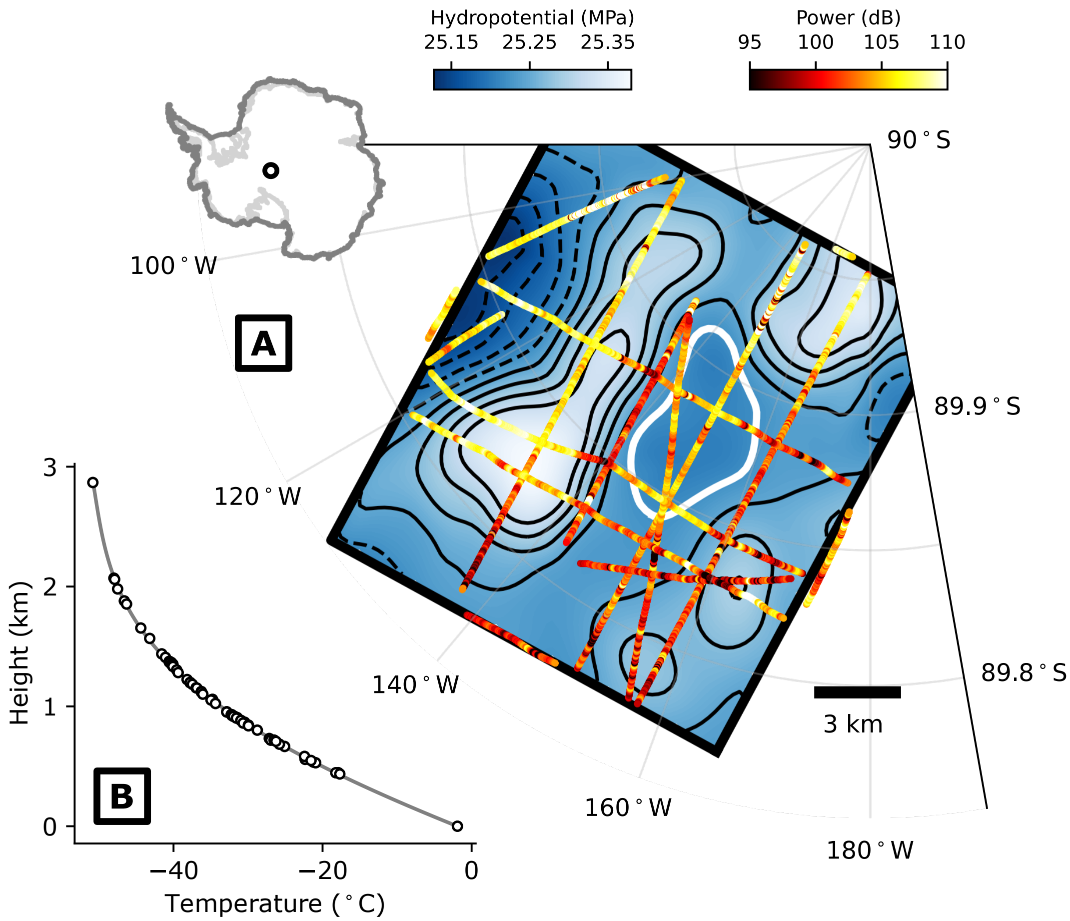

Figure 4: *Data and model summary of Study 2 – South Pole Lake. A) Map of SPL survey with the colormap showing hydropotential and the blue outline showing the lake area inferred by a hydropotential basin. Red dots show locations of ApRES acquisitions. Black vectors show GPS velocity measurements. B) Measured (Price et al., 2002) and modeled temperature profiles.*

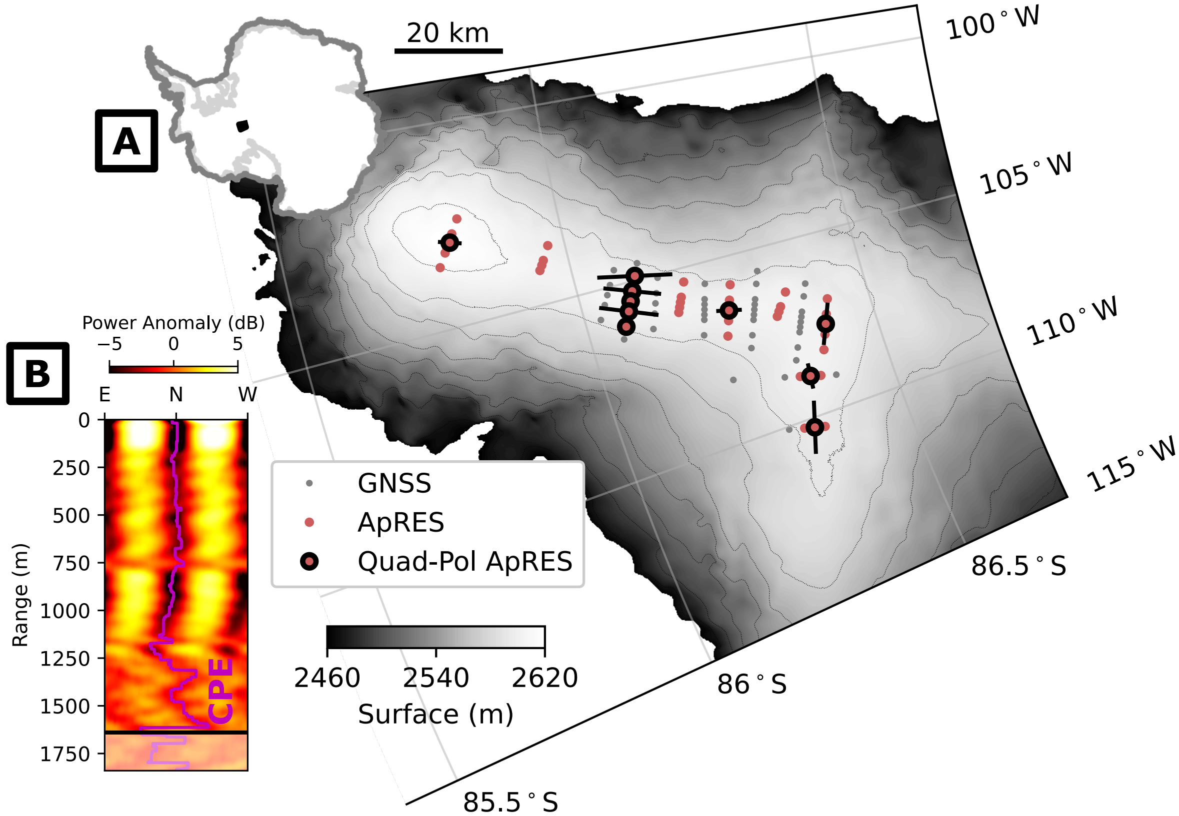

Figure 5: *Data and radar analysis summary of Study 3 – Hercules Dome. A) Map of HD survey with the colormap showing surface elevation from REMA (Howat et al., 2019), GNSS (grey), single-pol ApRES sites (red), and quad-pol ApRES sites (red with black bars at the inferred girdle axis). B) Cross-polarized power anomaly from one site with the cross-polarized extinction (CPE; magenta) being oriented at the girdle axis.*

Supplementary Work: *Numerical modeling of the Stefan Problem in cylindrical coordinates to aid design of a thermal melt probe (Hills et al., 2021).*

Data and Code Availability: *Data products will be made available through the UW Research Archive and USAP Data Center. The data from SPL have been archived, https://www.usap-dc.org/view/project/p0010160. Processing and modeling code are available at https://github.com/benhills.*

Funding: *Funding from NSF grants 1744649 and 1643353 as well as NASA grant NNX17AF68G. I will continue to be funded on grant 1744649 and possibly others.*

References

Alley, R.B., 1992. Flow-law hypotheses for ice-sheet modeling. J. Glaciol. 38.

Alley, R.B., 1988. Fabrics in Polar Ice Sheets: Development and Prediction. Science (80-.). 240, 493–495.

Azuma, N., 1994. A flow law for anisotropic ice and its application to ice sheets. Earth Planet. Sci. Lett. 128, 601–614. https://doi.org/10.1016/0012-821X(94)90173-2

Beem, L.H., Cavitte, M.G.P., Blankenship, D.D., Carter, S.P., Young, D.A., Muldoon, G.R., Jackson, C.S., Siegert, M.J., 2017. Ice-flow reorganization within the East Antarctic Ice Sheet deep interior. Geol. Soc. London Spec. Publ. 461. https://doi.org/10.1144/SP461.14

Bingham, R.G., Siegert, M.J., Young, D.A., Blankenship, D.D., 2007. Organized flow from the South Pole to the Filchner-Ronne ice shelf: An assessment of balance velocities in interior East Antarctica using radio echo sounding data. J. Geophys. Res. Earth Surf. 112, 1–11. https://doi.org/10.1029/2006JF000556

Brennan, P. V., Lok, L.B., Nicholls, K., Corr, H., 2014. Phase-sensitive FMCW radar system for high-precision antarctic ice shelf profile monitoring. IET Radar, Sonar Navig. 8, 776–786. https://doi.org/10.1049/iet-rsn.2013.0053

Brook, E.J., Nesje, A., Lehman, S.J., Raisbeck, G.M., Yiou, F., 1996. Cosmogenic nuclide exposure ages along a vertical transect in western Norway: Implications for the height of the Fennoscandian ice sheet. Geology 24, 207–210. https://doi.org/10.1130/0091-7613(1996)024<0207:CNEAAA>2.3.CO;2

Budd, W.F., Jacka, T.H., 1989. A review of ice rheology for ice sheet modelling.

Carter, S.P., Blankenship, D.D., Peters, M.E., Young, D.A., Holt, J.W., Morse, D.L., 2007. Radar-based subglacial lake classification in Antarctica. Geochemistry Geophys. Geosystems 8, 1–20. https://doi.org/10.1029/2006GC001408

Christianson, K., Jacobel, R.W., Horgan, H.J., Alley, R.B., Anandakrishnan, S., Holland, D.M., Dallasanta, K.J., 2016. Basal conditions at the grounding zone of Whillans Ice Stream, West Antarctica, from ice-penetrating radar. J. Geophys. Res. Earth Surf. 121, 1954–1983. https://doi.org/10.1002/2015JF003806

Christianson, K., Jacobel, R.W., Horgan, H.J., Anandakrishnan, S., Alley, R.B., 2012. Subglacial Lake Whillans - Ice-penetrating radar and GPS observations of a shallow active reservoir beneath a West Antarctic ice stream. Earth Planet. Sci. Lett. 331–332, 237–245. https://doi.org/10.1016/j.epsl.2012.03.013

Clarke, G.K.C., Nitsan, U., Paterson, W.S.B., 1977. Strain heating and creep instability in glaciers and ice sheets. Rev. Geophys. 15, 235. https://doi.org/10.1029/RG015i002p00235

Dahl-Jensen, D., 1998. Steady thermomechanical flow along two-dimensional flow lines in large grounded ice sheets. J. Geophys. Res. 94, 355–362.

Dahl-Jensen, D., Mosegaard, K., Gundestrup, N., Clow, G.D., Johnsen, S.J., Hansen, A.W., Balling, N., 1998. Past temperatures directly from the Greenland Ice Sheet. Science (80-.). 282, 268–271. https://doi.org/10.1126/science.282.5387.268

DeConto, R.M., Pollard, D., 2016. Contribution of Antarctica to past and future sea-level rise. Nature 531, 591–597. https://doi.org/10.1038/nature17145

Drews, R., Eisen, O., Steinhage, D., Weikusat, I., Kipfstuhl, S., Wilhelms, F., 2012. Potential mechanisms for anisotropy in ice-penetrating radar data. J. Glaciol. 58, 613–624. https://doi.org/10.3189/2012JoG11J114

Engelhardt, H., 2004. Thermal regime and dynamics of the West Antarctic ice sheet. Ann. Glaciol. Vol 39, 2005 39, 85–92.

Ershadi, M.R., Drews, R., Martín, C., Eisen, O., Ritz, C., Corr, H., Christmann, J., Zeising, O., Humbert, A., Mulvaney, R., 2021. Polarimetric radar reveals the spatial distribution of ice fabric at domes in East Antarctica. Cryosph. Discuss. 1–34.

Fox-Kemper, B., Hewitt, H.T., Xiao, C., Aðalgeirsdóttir, G., Drijfhout, S.S., Edwards, T.L., Golledge, N.R., Hemer, M., Kopp, R.E., Krinner, G., Mix, A., Notz, D., Nowicki, S., Nurhati, I.S., Ruiz, L., Sallée, J.-B., Slangen, A.B.A., Yu, Y., 2021. Ocean, Cryosphere and Sea Level Change Climate Change 2021: The Physical Science Basis. Contrib. Work. Gr. I to Sixth Assess. Rep. Panel Clim. Chang.

Fudge, T.J., Biyani, S.C., Clemens-Sewall, D., Hawley, R.L., 2019. Constraining Geothermal Flux at Coastal Domes of the Ross Ice Sheet, Antarctica. Geophys. Res. Lett. 46, 13090–13098. https://doi.org/10.1029/2019GL084332

Fujita, S., Maeno, H., Matsuoka, K., 2006. Radio-wave depolarization and scattering within ice sheets: A matrix-based model to link radar and ice-core measurements and its application. J. Glaciol. 52, 407–424. https://doi.org/10.3189/172756506781828548

Fujita, S., Matsuoka, T., Ishida, T., Matsuoka, K., Mae, S., 2000. A summary of the complex dielectric permittivity of ice in the megahertz range and its applications for radar sounding of polar ice sheets. Phys. Ice Core Rec. 185–212.
Glen, J.W., 1955. the Creep of Polycrystalline Ice. Proc. R. Soc. London A Math. Phys. Eng. Sci. 228, 519–538.
Harrington, J. a, Humphrey, N.F., Harper, J.T., 2015. Temperature distribution and thermal anomalies along a flowline of the Greenland Ice Sheet. Ann. Glaciol. 56, 98–104. https://doi.org/10.3189/2015AoG70A945
Harrison, W.D., Echelmeyer, K.A., Larsen, C.F., 1998. Measurement of temperature in a margin of Ice Stream B, Antarctica: implications for margin migration and lateral drag. J. Glaciol. 44, 615–624.
Hills, B.H., Christianson, K., Holschuh, N., 2020. A framework for attenuation method selection evaluated with ice-penetrating radar data at South Pole Lake. Ann. Glaciol. 61, 1–12. https://doi.org/10.1017/aog.2020.32
Hills, B.H., Winebrenner, D.P., Elam, W.T., Kintner, P.M.S., 2021. Avoiding slush for hot-point drilling of glacier boreholes. Ann. Glaciol. 62, 166–170. https://doi.org/10.1017/aog.2020.70
Holschuh, N., Christianson, K., Anandakrishnan, S., Alley, R.B., Jacobel, R.W., 2016. Constraining attenuation uncertainty in common midpoint radar surveys of ice sheets. J. Geophys. Res. F Earth Surf. 121, 1876–1890. https://doi.org/10.1002/2016JF003942
Holschuh, N., Lilien, D.A., Christianson, K., 2019. Thermal Weakening, Convergent Flow, and Vertical Heat Transport in the Northeast Greenland Ice Stream Shear Margins. Geophys. Res. Lett. 8184–8193. https://doi.org/10.1029/2019gl083436
Howat, I.M., Porter, C., Smith, B.E., Noh, M.-J., Morin, P., 2019. The Reference Elevation Model of Antarctica. Cryosph. 1–16. https://doi.org/10.5194/tc-2018-240
Iken, A., Echelmeyer, K., Harrison, W., Funk, M., 1993. Mechanisms of fast flow in Jakobshavns Isbrae, West Greenland: Part I. Measurements of temperature and water level in deep boreholes. J. Glaciol. 39, 15–25.
Jackson, M., Kamb, B., 1997. The marginal shear stress of Ice Stream B, West Antarctica. J. Glaciol. 43, 415–426.
Jacobel, R.W., Welch, B.C., Osterhouse, D., Pettersson, R., Macgregor, J.A., 2009. Spatial variation of radar-derived basal conditions on Kamb Ice Stream, West Antarctica. Ann. Glaciol. 50, 10–16. https://doi.org/10.3189/172756409789097504
Jacobson, H.P., Raymond, C.F., 1998. Thermal effects on the location of ice stream margins. J. Geophys. Res. 103. https://doi.org/10.1029/98JB00574
Jordan, T.M., Schroeder, D.M., Castelletti, D., Li, J., Dall, J., 2019. A Polarimetric Coherence Method to Determine Ice Crystal Orientation Fabric from Radar Sounding: Application to the NEEM Ice Core Region. IEEE Trans. Geosci. Remote Sens. 57, 8641–8657. https://doi.org/10.1109/TGRS.2019.2921980
Jordan, T.M., Schroeder, D.M., Cooper, W., Siegfried, M.R., 2020. Estimation of ice fabric within Whillans Ice Stream using polarimetric phase-sensitive radar sounding 00, 1–24.
Kahle, E.C., Steig, E.J., Jones, T.R., Fudge, T.J., Koutnik, M.R., Morris, V.A., Vaughn, B.H., Schauer, A.J., Stevens, C.M., Conway, H., Waddington, E.D., Buizert, C., Epifanio, J., White, J.W.C., 2021. Reconstruction of Temperature, Accumulation Rate, and Layer Thinning From an Ice Core at South Pole, Using a Statistical Inverse Method. J. Geophys. Res. Atmos. 126, 1–20. https://doi.org/10.1029/2020jd033300
Lilien, D.A., Fudge, T.J., Koutnik, M.R., Conway, H., 2018. Holocene Ice-Flow Speedup in the Vicinity of the South Pole. Geophys. Res. Lett. 45, 6557–6565. https://doi.org/10.1029/2018GL078253
Lilien, D.A., Hills, B.H., Driscol, J., Jacobel, R., Christianson, K., 2020. ImpDAR: An open-source impulse radar processor. Ann. Glaciol. 61, 114–123. https://doi.org/10.1017/aog.2020.44
Lliboutry, L., 1979. A critical review of analytical approximate solutions for steady state velocities and temperatures in cold ice-sheets. Gletscherkd. Glazialgeol. 15, 135–148.
Lliboutry, L., 1968. General Theory of Subglacial Cavitation and Sliding of Temperate Glaciers. J. Glaciol. 7, 21–58. https://doi.org/10.1017/S0022143000020396
MacGregor, J.A., Fahnestock, M.A., Catania, G.A., Paden, J.D., Gogineni, S.P., Young, S.K., Rybarski, S.C., Mabrey, A.N., Wagman, B.M., Morlighem, M., 2015a. Radiostratigraphy and age structure of the Greenland Ice Sheet. J. Geophys. Res. Earth Surf. 120, 212–241. https://doi.org/10.1002/2014JF003215.Received
MacGregor, J.A., Li, J., Paden, J.D., Catania, G. a, Clow, G.D., Fahnestock, M. a, Gogineni, S.P., Grimm, R.E., Morlighem, M., Nandi, S., Seroussi, H., Stillman, D.E., 2015b. Radar attenuation and temperature within the Greenland Ice Sheet. J. Geophys. Res. Earth Surf. 120, 983–1008. https://doi.org/10.1002/2014JF003418
MacGregor, J.A., Winebrenner, D.P., Conway, H., Matsuoka, K., Mayewski, P.A., Clow, G.D., 2007. Modeling englacial radar attenuation at Siple Dome, West Antarctica, using ice chemistry and temperature data. J. Geophys. Res. Earth Surf. 112, 1–14. https://doi.org/10.1029/2006JF000717
Meyer, C.R., Minchew, B.M., 2018. Temperate ice in the shear margins of the Antarctic Ice Sheet: Controlling processes and preliminary locations. Earth Planet. Sci. Lett. 498, 17–26. https://doi.org/10.1016/j.epsl.2018.06.028
Mouginot, J., Rignot, E., Scheuchl, B., 2019. Continent-Wide, Interferometric SAR Phase, Mapping of Antarctic Ice Velocity. Geophys. Res. Lett. 46, 9710–9718. https://doi.org/10.1029/2019GL083826
Nicholls, K.W., Corr, H.F.J., Stewart, C.L., Lok, L.B., Brennan, P. V., Vaughan, D.G., 2015. Instruments and methods: A ground-based radar for measuring vertical strain rates and time-varying basal melt rates in ice sheets and shelves. J. Glaciol. 61, 1079–1087. https://doi.org/10.3189/2015JoG15J073
Perol, T., Rice, J.R., 2015. Shear heating and weakening of the margins of Western Antarctic ice streams. Geophys. Res. Lett.

42, 3406–3413. https://doi.org/10.1002/2015GL063638.Received
Peters, L.E., Anandakrishnan, S., Holland, C.W., Horgan, H.J., Blankenship, D.D., Voigt, D.E., 2008. Seismic detection of a subglacial lake near the South Pole , Antarctica. Geophys. Res. Lett. 35, 1–5. https://doi.org/10.1029/2008GL035704
Phillips, T., Rajaram, H., Steffen, K., 2010. Cryo-hydrologic warming: A potential mechanism for rapid thermal response of ice sheets. Geophys. Res. Lett. 37, 1–5. https://doi.org/10.1029/2010GL044397
Price, P.B., Nagornov, O. V, Bay, R., Chirkin, D., He, Y., Miocinovic, P., Richards, A., Woschnagg, K., Koci, B., Zagorodnov, V., 2002. Temperature profile for glacial ice at the South Pole : Implications for life in a nearby subglacial lake. Proc. Natl. Acad. Sci. 99, 7844–7847. https://doi.org/10.1073/pnas.082238999
Raymond, C.F., 1983. Deformation in the vicinity of ice divides. J. Glaciol. 29, 357–373. https://doi.org/10.3189/S0022143000030288
Rignot, E., Jacobs, S., Mouginot, J., Scheuchl, B., 2013. Ice-shelf melting around antarctica. Science (80-.). 341, 266–270. https://doi.org/10.1126/science.1235798
Robin, G. de Q., 1955. Ice movement and temperature distribution in glaciers and ice sheets. J. Glaciol. 2, 523–532.
Schroeder, D.M., Seroussi, H., Chu, W., Young, D.A., 2016. Adaptively constraining radar attenuation and temperature across the Thwaites Glacier catchment using bed echoes. J. Glaciol. 62, 1075–1082. https://doi.org/10.1017/jog.2016.100
Shoji, H., Langway, C.C., 1988. Flow-Law Parameters of the Dye 3, Greenland, Deep Ice Core. Ann. Glaciol. 10, 146–150. https://doi.org/10.3189/s026030550000433x
Smith, E.C., Baird, A.F., Kendall, J.M., Martín, C., White, R.S., Brisbourne, A.M., Smith, A.M., 2017. Ice fabric in an Antarctic ice stream interpreted from seismic anisotropy. Geophys. Res. Lett. 44, 3710–3718. https://doi.org/10.1002/2016GL072093
Steig, E.J., Huybers, K., Singh, H.A., Steiger, N.J., Ding, Q., Frierson, D.M.W., Popp, T., White, J.W.C., 2015. Influence of West Antarctic Ice Sheet collapse on Antarctic surface climate. https://doi.org/10.1002/2015GL063861.Abstract
Suckale, J., Platt, J.D., Perol, T., Rice, J.R., 2014. Earth Surface Deformation-induced melting in the margins of the West Antarctic ice streams. J. Geophys. Res. Earth Surf. 119, 1004–1025. https://doi.org/10.1002/2013JF003008.Flow
Venturelli, R.A., Siegfried, M.R., Roush, K.A., Li, W., Burnett, J., Zook, R., Fricker, H.A., Priscu, J.C., Leventer, A., Rosenheim, B.E., 2020. Mid-Holocene Grounding Line Retreat and Readvance at Whillans Ice Stream, West Antarctica. Geophys. Res. Lett. 47. https://doi.org/10.1029/2020GL088476
Weertman, J., 1968. Comparison between Measured and Theoretical Temperature Profiles of the Camp Century, Greenland, Borehole. J. Geophys. Res. 73, 2691–2700. https://doi.org/10.1029/JB073i008p02691
Weertman, J., 1957. On the sliding of glaciers. J. Glaciol. 3, 33–38. https://doi.org/10.3189/S002214300002470
Welch, B.C., Jacobel, R.W., 2005. Bedrock topography and wind erosion sites in East Antarctica: Observations from the 2002 US-ITASE traverse. Ann. Glaciol. 41, 92–96. https://doi.org/10.3189/172756405781813258
Welch, B.C., Jacobel, R.W., 2003. Analysis of deep-penetrating radar surveys of West Antarctica, US-ITASE 2001. Geophys. Res. Lett. 30. https://doi.org/10.1029/2003GL017210
Young, T.J., Martín, C., Christoffersen, P., Schroeder, D.M., Tulaczyk, S.M., Dawson, E.J., 2021. Rapid and accurate polarimetric radar measurements of ice crystal fabric orientation at the Western Antarctic Ice Sheet (WAIS) Divide ice core site. Cryosphere 15, 4117–4133. https://doi.org/10.5194/tc-15-4117-2021